World of Science: Journal on Modern Research Methodologies

Volume 2 Issue 5, Year 2023
ISSN: 2835-3072
https://univerpubl.com/index.php/woscience

A Computer-Aided Study of Bipolar Magnetic Lenses

Ibtihal Mohammed , Gaber FAISEL
Süleyman Demirel Üniversitesi, Türkiye
Email : ebtmom3@gmail.com ; gaber_faisel@yahoo.com

Article Information

Received: March 03, 2023
Accepted: April 05, 2023
Published: May 07, 2023

Keywords
Magnetic electron lens, focal length, spherical aberration

ABSTRACT
In this research, I designed and studied the optical properties of electromagnetic electronic lenses of the bipolar type, as the effect of the axial aperture diameter of these lenses was studied on the objective focal length and coefficients of spherical and chromatic aberration, using a computer program (EOD) asymmetric. It was found that the objective optical properties improved significantly the lower the values of the diameter of the axial aperture of these

All electron-optical systems employ electron lenses, which are the most widely used and important part of the electron microscope. The electromagnetic lens, sometimes called the magnetic lens, the permanent magnet lens, and the electrostatic or electric lens are the three primary variants of this lens. The latter kind is employed more frequently in commerce than the former varieties due to its simple and exact function, ease of fabrication, and inexpensive cost. However, the electron lens has a number of "aberrations" that reduce its effectiveness. These aberrations arise from the fact that the lens system is unable to focus a charged particle beam from a single point in the object plane onto a single point in the Gaussian image plane. The image will consequently appear warped or fuzzy. The effectiveness of charge particle optical systems is consequently decreased by these flaws. Numerous solutions to the issue, including the so-called optimization, have been developed in response to the challenge of developing an aberration-free lens system.Two extremely distinct optimization strategies are ANALYSIS and SYNTHESIS. 2The latter involves the creation of a tool to satisfy a set of performance requirements [1]. In the first, the designer begins by calculating the lens' optical properties. The physical and geometrical features of the suggested design must be altered if the results are unsatisfactory from an electron-optics perspective. Until the desired results are attained, the process is repeated. As a result, a lot of this process is trial and error. The practice of optimization through analysis has gained popularity since the middle of the previous century. The effects of pole piece saturation on the focal characteristics of the objective lens [4] and the effects of the axial magnetic field distribution on the asymmetrical objective lens with high voltage electron microscopy [5,6] are two analysis-related concepts that have since been adopted. The goal of the current experiment is to develop and study an asymmetrical magnetic lens by altering important geometrical parameters, which is being done via the EOD software [15].

2. Analysis using finite elements and EOD software

Lencova [15] created the EOD program, which enables users to create complex electron lens

structures and do very precise computations of their magnetic field distribution and optical characteristics. In this application, regardless of the geometry of their pole components, all magnetic lenses are investigated using the finite element method (FEM), a computer technique. The first presentation of it in the area of electron optics was made by Munro [14]. This makes it possible to calculate the magnetic fields of spherical and electrostatic lenses two different types of lenses with many uses in physics and engineering exactly.

3. Lens design

Figure 1 illustrates the dimensions and grid-lines distribution (mesh) of the lens that were established using FEM in order for the EOD [15] program to compute the axial magnetic-field distribution of the lens and its related objective characteristics. Two soft iron magnetic pole elements, each with a D=6 mm diameter, make up the lens. These components are housed inside a circular coil with a cross-sectional area of 0.741mm2. The "action region," which has a thickness of S=6mm, is where most of the magnetic flux is concentrated. To prevent magnetic field leakage outside the lens, a soft iron circuit surrounds the coil and the magnetic polepieces.

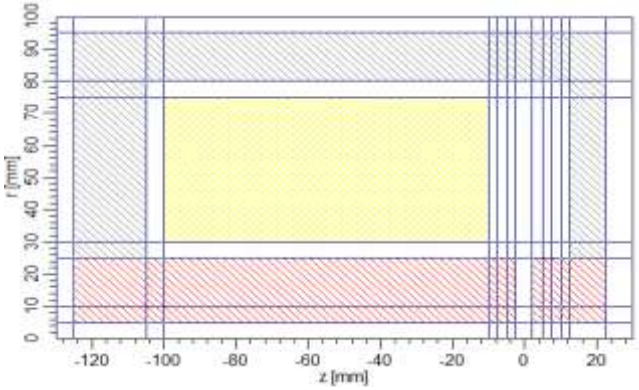

Fig 1: asymmetrical magnetic lens components in the upper half.

In Figure 2, the asymmetrical magnetic lens' geometrical arrangement and magnetic flux line dispersion are depicted. Knowing N, the total number of turns in the energizing coil carrying a current I, is necessary to calculate the axial flux density for constant lens excitation (NI=3000 A.t). 0.741 A/mm2 is the current density.

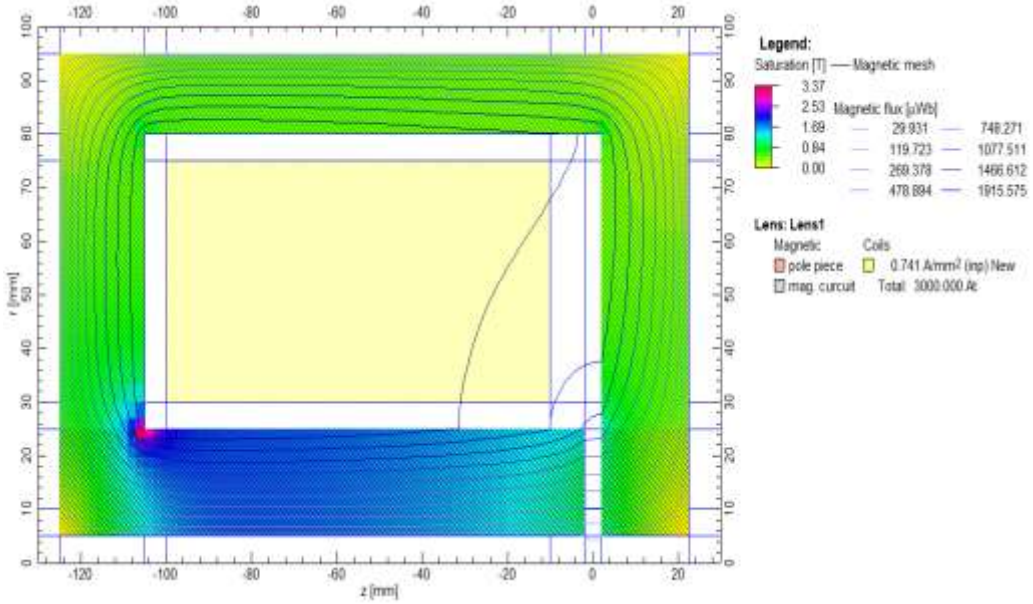

Fig: 2 With magnetic flux line distribution, the proposed asymmetric lens's upper half is geometrically designed..

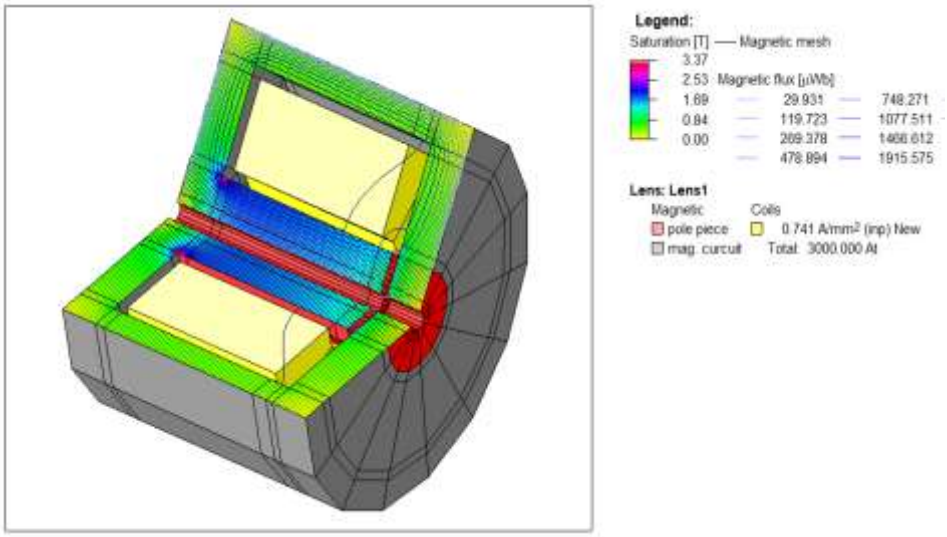

Fig. 3 shows a three-dimensional portion of the lens for better presentation.

4. Evaluation of properties

The spherical and chromatic aberration coefficients are usually acknowledged as the main factors limiting an objective lens's resolution. The chromatic C_C and spherical C_S aberration coefficients for the current experiment were determined using [14].

T $$C_S = \left[\frac{\eta}{128V_r}\right]\int_{z_1}^{z_2}\left[\left(\frac{3\eta}{V_r}\right)B_z^4 r_\alpha^4 + 8B_z'^2 r_\alpha^4 - 8B_z^2 r_\alpha^2 r_\alpha'^2\right]dz \quad (1)$$ and radial D_R

d

w $$C_C = \left[\frac{\eta}{8V_r}\right]\int_{z_1}^{z_2} B_z^2\, r_\alpha^2 dz \quad (2)$$ distortions,

$$D_r = \left[\frac{\eta}{128V_r}\right]\int_{z_1}^{z_2}\left[\left(\frac{\eta}{V_r}B_z + 8B_z''\right)r_\alpha r_\gamma^3 - 4B_z''\left(r_\gamma'' r_\alpha r_\gamma + r_\gamma' r^2 r_\alpha'\right)\right]dz \quad (3)$$

$$D_S = \int_{z_1}^{z_2}\left[\frac{3}{128}\left(\frac{\eta}{V_r}\right)^{\frac{3}{2}} r_\alpha^2 B_z^2 + \frac{1}{16}\left(\frac{\eta}{V_r}\right)^{\frac{1}{2}} r_\alpha'^2 B_Z\right]dz \quad (4)$$

The axial positions at which the magnetic field vanishes, η are z_1 and z_2, is the electron charge-to-mass ratio, and V_r is the relativity-adjusted accelerating voltage. The first and second derivatives of the axial magnetic flux density distribution are denoted by the abbreviations by B'_Z, B''_Z, respectively, and the paraxial-ray equation (5)'s solution is denoted by r_α.

The paraxial ray equation is used to determine $B_Z(z)$, which must be calculated in order to determine C_S, C_C, D_r, and D_S, respectively.

$$r''(z) + \frac{\eta}{8v_r} + B_Z^2 r(z) = 0 \quad (5)$$

Used It should be emphasized that during the course of the current inquiry, the derivatives and integrals were analyzed using Simpson's rule and the cubic spline differentiation method.

5. Results and discussion

5.1. The axial bore D

Since D has a significant impact on the magnetic field's strength, its impact on the optical properties is first examined. While maintaining the air gap constant at S=6 mm, four different values of D, ranging from 2 to 8 mm, have been used (see Table 1). Geometric patterns and B(z) designs for various values of D are displayed in Figs. 4 and 5, respectively. Although the half-width W of B_Z (z) rises, the maximum magnetic field B_{max} appears to decrease as D increases..

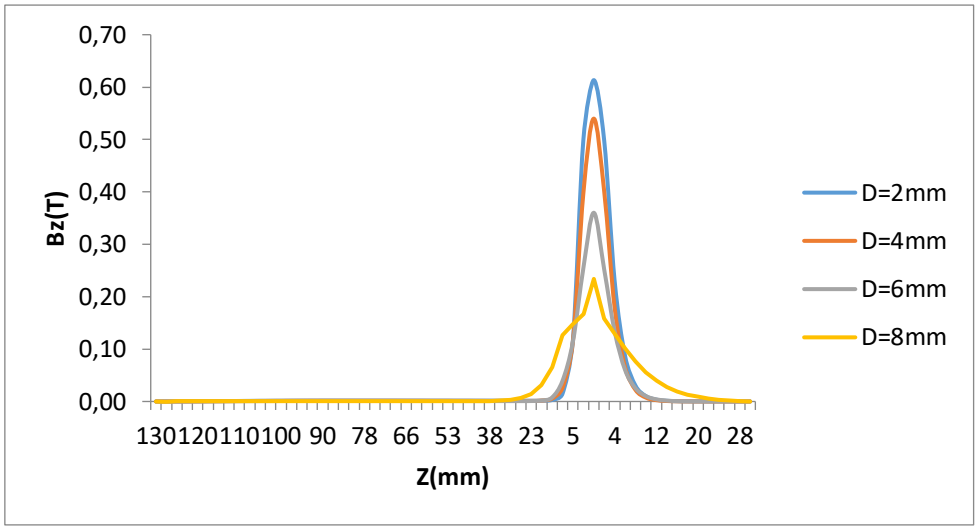

Fig. 4: The B_Z (Z) magnetic field distribution for various D values.

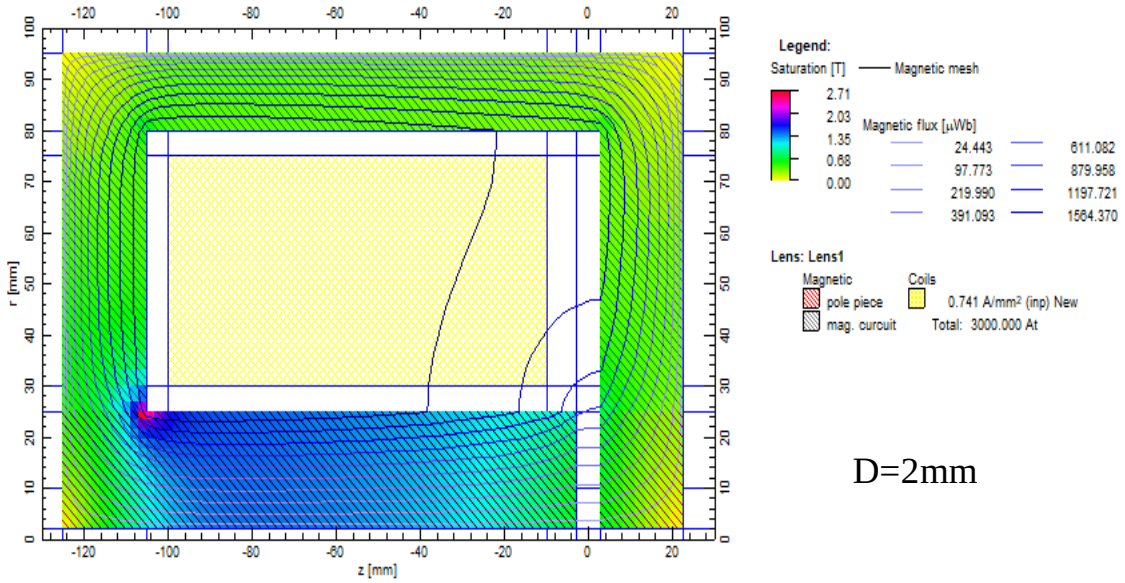

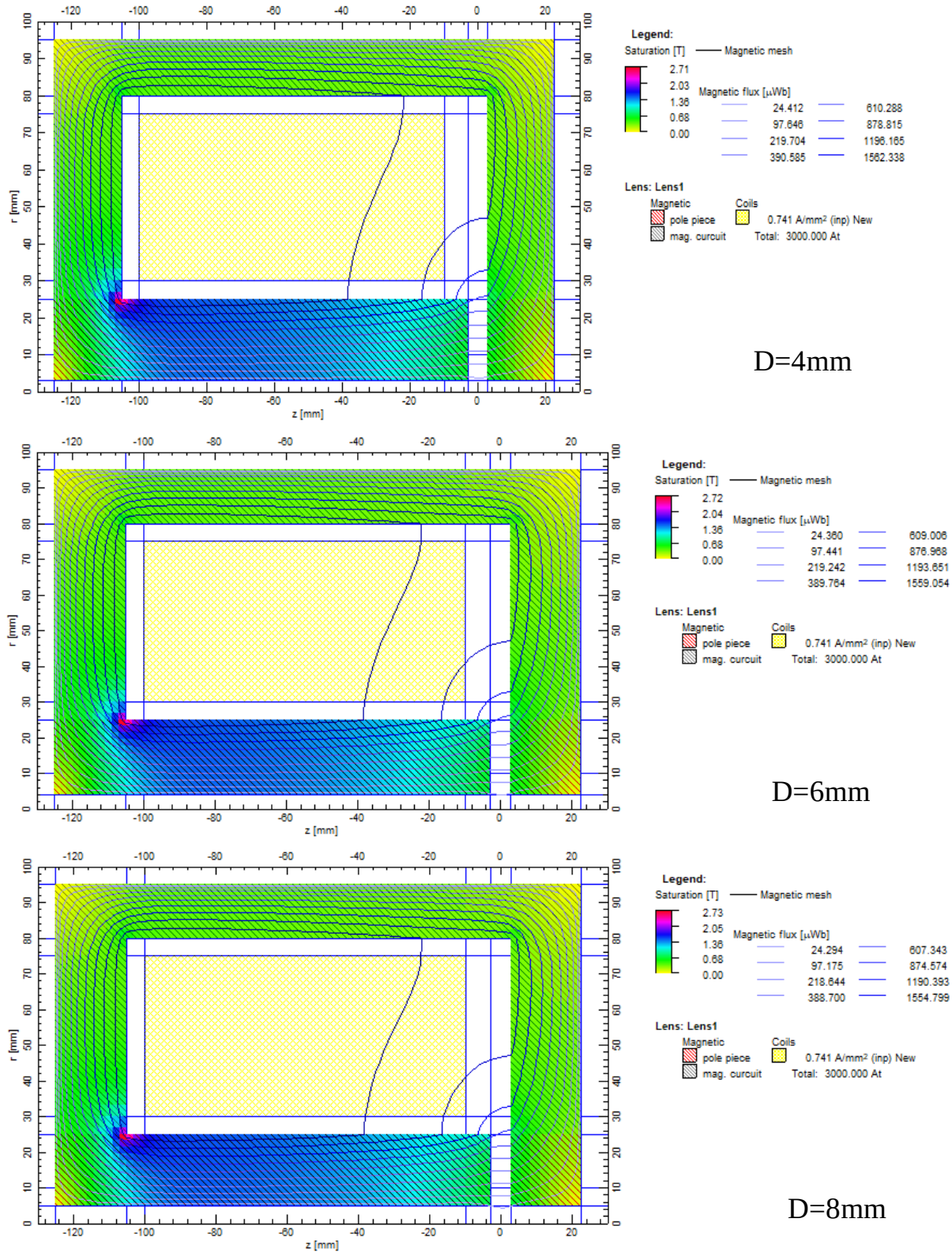

Fig. 5 Designs of the Upper Half of the Lens in Different D Values.

The objective optical characteristics are measured at NI/Vr =8, which is the typical operating point for objective lenses [20].

The focal length f_o, C_S, and C_C are observed to noticeably deteriorate as D is raised by changing the axial bores of the pole piece, as shown in Table 1.

Table 1: Comparing the Deduced Imaging Fields' Objective Optical Properties to the Parameter D at NI/√VR= 8

D(mm)	C_C(mm)	C_S(mm)	F_o(mm)
2	3.625 2.549	3.521 2.670	2.177
4	2.271	1.877	3.090
6	2.036	1.338	4.234
8			5.466

The projector optical properties, on the other hand, are listed in Table 2 for the projector focal length (f_P)min minimum value, and D_r and D_s rapidly improve as D increases.

Table2: Projector Optical Properties Against the Parameter D for the Deduced Imaging Fields at the Lowest Value of F_P

D(mm)	$(f_P)_{min}$	D_r (1/mm^2)	D_S(1/mm^2)
2	2.755	0.0080	0.081
4	4.5321	0.0074	0.060
6	6.232	0.0050	0.040
8	7.582	0.0031	0.018

5.2. Air gap S

At constant D = 6 mm, Tables 3 and 4 illustrate how S affects the objective and projector properties, respectively. It is obvious that an alteration in S has a major impact on the imaging field's characteristics. The bigger action zone in Figure 6 and the ensuing lens power loss can be utilized to explain this phenomena. While the smallest D and S values produce the best (lowest) values of the objective focal characteristics, the largest D and S values produce the best projector features.

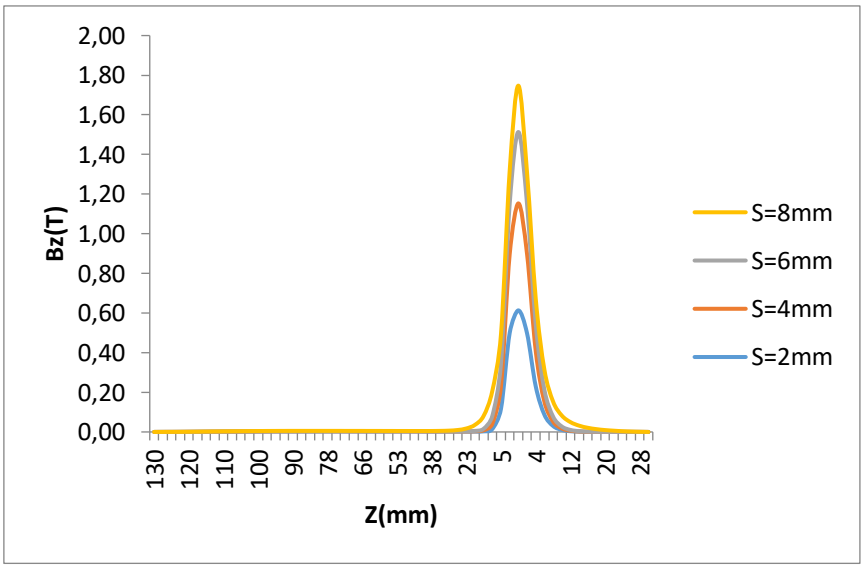

Fig. 6 B_Z Magnetic Field Distribution at Different S Values

Table 3 Optical Characteristics for the Deduced Imaging Fields in the Objective at NI/VR=8 against the S

S(mm)	(fp)min (mm)	Dr (1/mm2)	Ds (1/mm2)
2	2.6408	0.040	0.098
4	3.5819	0.006	0.055
6	5.5940	0.004	0.031
8	7.6504	0.003	0.019

Fig.7 magnetic flux patterns at various S values serve as an illustration of the geometrical layouts

for the proposed lens. At the smallest value of S=6 mm, this graph shows the increase in magnetic flux density.

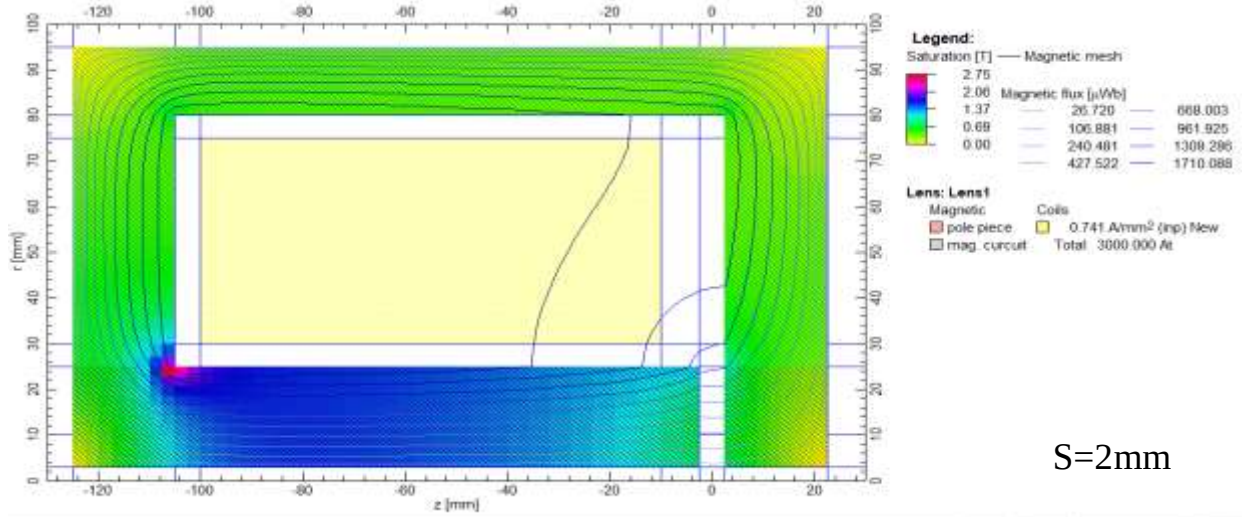

S=2mm

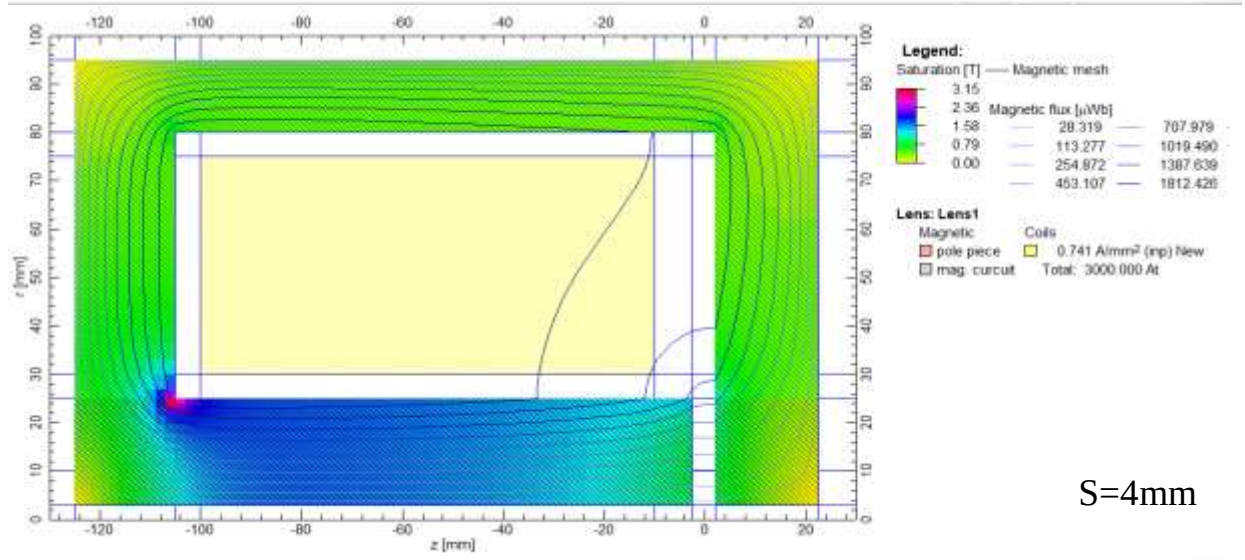

S=4mm

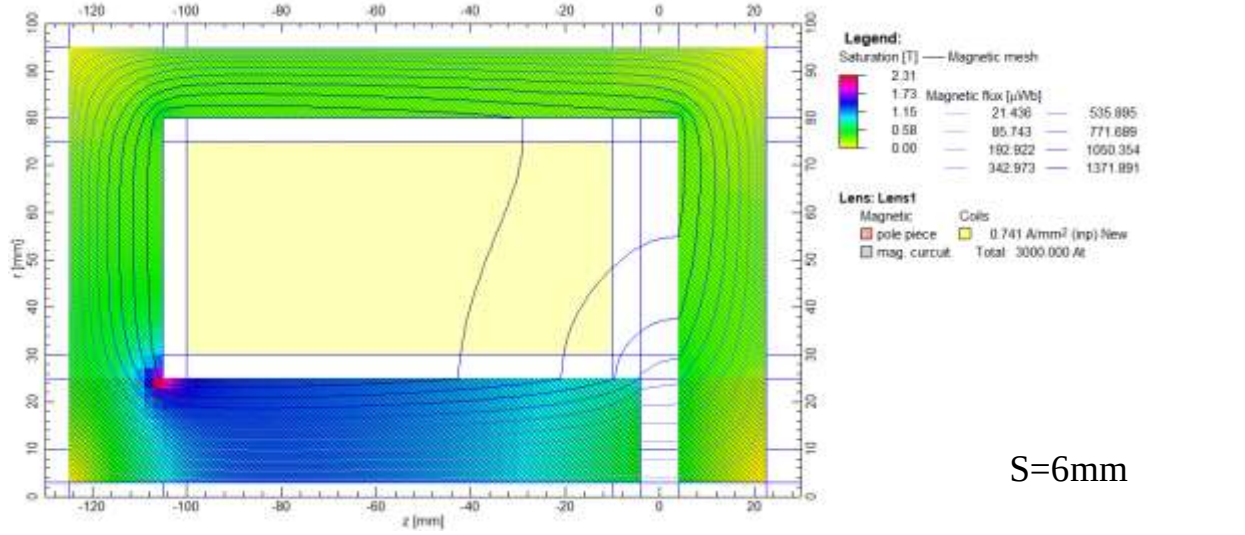

S=6mm

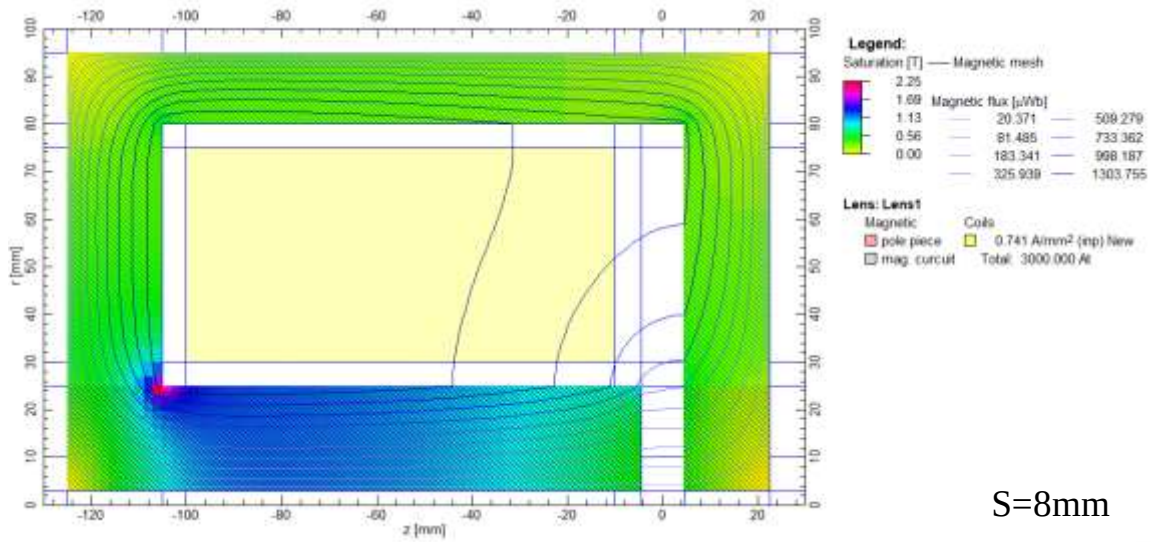

Fig. 7 Geometric Design of the Upper Half of the Lens for Different S Values.

6. Conclusion

The air gap and each of the pole components' axial bores contribute significantly to the best design of the asymmetrical magnetic lens, according to the findings of the current study. There is a significant difference between each of their effects, and the air gap clearly shows the greater one. While D and S were reduced, the objective focal properties improved significantly, though at a slower rate than the projector properties. In light of this, the EOD program can be regarded as a useful tool for obtaining the best asymmetrical magnetic lenses with great accuracy.

REFERENCES

1. Moses, R.W. Lens Optimization by Direct Application of the Cal-culus of Variation. Image Processing and Computer Aided Design in Electron Optics, ed. P.W. Hawkes (Academic Press). (1973)250-272.
2. Wasan J. Kadhem, Hassan N. Al-Obaidi. An Inverse Design Ap-proach For Magnetic Lenses Operated Under Infinite Magnification Condition. Optik 124 (2013)3523-3526. https://doi.org/10.1016/j.ijleo.2012.12.001.
3. Wasan J. Kadhem. Obtaining doublet magnetic lenses by synthesis technique. Optik 126 (2015) 40664071.https://doi.org/10.1016/j.ijleo.2015.07.204.
4. Kamminga, W. Properties of Magnetic Objective Lenses with Highly Saturated Polepieces. Optik 45(1976)39-54.
5. Tsuno, K. and Harada, Y., Elimination of Spiral Distortion in Elec-tron Microscopy Using an Asymmetrical Triple-Polepiece Lens. J. Phys. E: Sci. Instrum, 14 (1981b) 955-959. https://doi.org/10.1088/0022-3735/14/8/015.
6. Tsuno, K. and Honda, T., Magnetic Field Distribution and Optical Properties of Asymmetrical Objective Lenses For an Atomic Reso-lution High Voltage Electron Microscope. Optik 64 (1983) 367-78.

7. Zeitler, E., Analysis of an Imaging Magnetic Energy Filter, Nucl. Inst. Meth. Phys. Res. A, 298 (1990) 234-246. https://doi.org/10.1016/0168-9002(90)90621-C.
8. Szilagyi, M., Reconstruction of Electron and Polepiece From Opti-mized Axial Field Distribution of Electron and Ion Optical System. Appl. Phys. Lett., 45 (1984) 499-501. https://doi.org/10.1063/1.95315.
9. Szilagyi, M., Synthesis of Electron and Ion Optical Columns, J. Vac. Sci. Technol. 9 (1991) 2618-2621. https://doi.org/10.1116/1.585659.
10. Preikszas, D. and Rose, H., Procedures For Minimizing The Aber-rations of Electromagnetic Compound Lenses, Optik 100 (1995) 179-187.
11. Lencova, B., Accurate Computation of Magnetic Lenses with FO-FEM. Nucl. Inst. In addition, Meth. Phys. Res. A, 427 (1999) 329-337.
12. Juma, S. M., and Yahya, A. A., Focal Properties of Unsaturated Asymmetrical Magnetic Electron Lenses. J. Phys. E: Sci. Instrum., 19 (1986) 614-624. https://doi.org/10.1088/0022-3735/19/8/007.
13. Tsuno, K. and Honda, T., Magnetic Field Distribution and Optical Properties of Asymmetrical Objective Lenses For an Atomic Reso-lution High Voltage Electron Microscope. Optik 64 (1983)367-78.
14. Munro, E., A set of Computer Programs for Calculating the Proper-ties of Electron Lenses. University of Cambridge, Department of Engineering Report CUED/B-Elect. TR 45 (1975).
15. Lencova, B. Software for particle optics computation, http://www.lencova.com. 2009.
16. Munro, E., Computer-Aided Design of Electron Lenses by the Fi-nite Element Method. Image Processing and Computer-Aided De-sign in Electron Optics, ed. P. W. Hawkes (Academic Press) (1973) 284-323.
17. Szilagyi, M., Electron and Ion Optics, (Plenum Press: New York). (1988). https://doi.org/10.1007/978-1-4613-0923-9.
18. Lence, M. and Lencova, B., Saturated Single Polepiece Objective Lenses. Electron Microscopy, 1984 eds., A Csanady, R. Rohlich and Szaba (Programme Committee of the Eighth European Con-gress on Electron Microscopy, Budapest) (1984) 27-8.
19. Tsuno, K. and Harada, Y., Minimization of Radial and Spiral Dis-tortion in Electron Microscopy Through The Use of A Triple-Polepiece Lens, J. Phys. E: Sci. Instrum., 14 (1981a) 313-319. https://doi.org/10.1088/0022-3735/14/3/013.
20. Hawkes, P. W., Magnetic Electron Lenses. (Springer-verlag). (1982). https://doi.org/10.1007/978-3-642-81516-4.